Electron Paramagnetic Resonance Spectra Simulation Directly from Molecular Dynamics Trajectories of a Liquid Crystal with a Doped Paramagnetic Spin Probe

V. S. Oganesyan,* E. Kuprusevicius, H. Gopee, and A. N. Cammidge
School of Chemical Sciences and Pharmacy, University of East Anglia, Earlham Road, Norwich, NR4 7TJ, United Kingdom

M. R. Wilson
Department of Chemistry, University Science Laboratories, South Road, Durham, DH1 3LE, United Kingdom
(Received 10 October 2008; published 8 January 2009)

We report simulation of EPR spectra directly and entirely from trajectories generated from molecular dynamics simulations. Results are reported for a model 3β-DOXYL-5α-cholestane spin probe in a coarse-grained solvent representing a 5CB nematic host. The results are in excellent agreement with the experimental spectra. The calculated order parameters associated with the paramagnetic probe show strong correlation with the order parameter of 5CB mesogens and are in agreement with those reported in the literature. Simulation of EPR spectra entirely from molecular dynamics of real structures provides direct correlation between molecular motions and the features observed in the spectra, allowing unambiguous interpretation of the spectra. This method opens the possibility for ''computer engineering'' of spin-labeled materials with the desired properties, such as spin-labeled proteins, prior to experiment.

DOI: 10.1103/PhysRevLett.102.013005 PACS numbers: 33.35.+r, 61.30.−v, 64.70.mj, 76.30.−v

Multifrequency EPR spectroscopy has been developed into a valuable probe of dynamics and order, with wide applicability, by the use of nitroxide spin labels as paramagnetic probes [1]. EPR of spin probes has been used to test structural properties and molecular mobility of numerous complex molecular systems such as proteins and protein-protein complexes, DNA or RNA, polymers, lipids, nanostructures, monolayers at oil-water interfaces, and also liquid crystals (LC) [2–10].

Molecular modeling has been successfully used to complement various spectroscopic techniques, particularly NMR [11]. However, its application to EPR has been limited so far. For liquid crystals, despite the use of both atomistic and coarse-grained (CG) models to study phase behavior [11,12], no molecular dynamics (MD) calculations have been attempted for systems doped with paramagnetic spin probes. For other systems no simulations of spectra have been achieved directly and entirely from MD trajectories necessitating the use of additional modeling with adjustable parameters [13,14]. The major obstacle is that simulation of EPR spectra requires long dynamical trajectories of several microseconds to ensure a proper Fourier integration of the time-domain EPR signal. MD trajectories generated by modern computers are still too short for this purpose [15,16]. The need for dynamical trajectories substantially longer than those attainable by MD calculations imposes a major challenge and inevitably requires additional theoretical modeling with adjustable parameters with the fitting of experimental spectra as an inevitable requirement.

Recently, a novel simple and effective approach to the simulation of continuous wave (cw) EPR spectra has been developed that requires only short trajectories generated over the decay time of the autocorrelation function of the spin label motion [17]. The procedure covers the entire motional range of spin label. This approach is based on the fact that the time scale of the spin label motion is much shorter than the sampling time required to achieve an adequate resolution in the frequency domain after Fourier transformation [15,16]. Therefore, all the information required to simulate EPR spectra should be contained in the sampling trajectory on the much shorter time scale of the correlation time of the spin-label orientations (nanoseconds range), the decay time of the autocorrelation function ($\sim 10\tau_c$). These times can (easily) be accessed by modern MD simulation methods. This Letter reports the first successful simulation of EPR spectra directly from a single MD trajectory of spin probe introduced within a CG model of the nematogen 5CB at different temperatures.

Following Robinson *et al.* [15] and Steinhoff and Hubbell [18], EPR spectra are calculated as Fourier transforms of statistically averaged transverse magnetization curves for each of the three hyperfine lines of a nitroxide spin label, which are described by the following formal solution:

$$\langle M_+^m(t)\rangle = \langle M_+^m(0)\rangle \left\langle \exp\left\{-\left[i\int_0^t \omega^m(\tau)d\tau + \frac{t}{T_2^m}\right]\right\}\right\rangle. \quad (1)$$

Here $\langle\cdots\rangle$ indicates the ensemble average, and the Larmor frequencies for the three hyperfine lines $\omega^m(t)$ are the functions of the orientation trajectory $\Omega(t)$ according to

$$\omega^m(t) = \{g_{ZZ}[\Omega(t)]\beta B + A_{ZZ}[\Omega(t)]m\}/\hbar. \quad (2)$$

B is the value of magnetic field, m is the projection of the nitrogen nuclear spin on its quantization axis, which for

^{14}N is equal to $\pm 1, 0$. g_{ZZ} and A_{ZZ} are effective g and hyperfine coupling constants, respectively. A_{ZZ} is calculated in accordance with the procedure introduced by Steinhoff and Hubbell [18] in order to account for the effects of pseudosecular terms in the slow motional limit. In order to account for homogeneous line broadening of the EPR spectrum, the transverse relaxation time T_2^m is introduced. The following procedure is then used to calculate the EPR spectra from a single MD trajectory.

(1) A single trajectory is calculated for the time interval T_r, long enough (normally up to several ns) to allow a statistical average of $\langle M_+^m(t)\rangle$ to be performed using a ''sliding time window'' technique [16]. For this time interval the evolution of $\langle M_+^m(t)\rangle$ for each initial orientation relative to magnetic field is calculated numerically recursively [17].

(2) After the autocorrelation function of the spin probe's motion has completely relaxed ($t \geq T_r$) the rest of magnetization trajectory for the entire sampling time is calculated according to

$$\langle M_+^m(t)\rangle = \langle M_+^m(T_r)\rangle \exp\left[-\left(i\bar{\omega}^m + \lambda^m + \frac{1}{T_2^m}\right)(t - T_r)\right], \tag{3}$$

where for each hyperfine line m,

$$\bar{\omega}^m = \frac{1}{T_r}\int_0^{T_r}\langle\omega^m(\tau)\rangle d\tau \tag{4}$$

and

$$\lambda^m = \int_0^{T_r}\langle\Delta\omega^m(0)\Delta\omega^m(\tau)\rangle d\tau \tag{5}$$

are the stationary limit reached by the statistically averaged frequency and the so-called dephasing rate, respectively. The dephasing of magnetizations is caused by the modulation due to the reorientational dynamics of the spin probe. In the above, $\langle\Delta\omega^m(0)\Delta\omega^m(\tau)\rangle$ are autocorrelation functions of $\Delta\omega^m(t) = \omega^m(t) - \bar{\omega}^m(t)$.

(3) Finally, the Fourier transform of each trajectory provides the contribution to the EPR spectrum. The total line shape intensity must be averaged over all possible orientations of the director. The correlation time required to provide an estimate of T_r is defined as [16]

$$\tau_c = \int_0^\infty \frac{C(t)}{C(0)}dt, \tag{6}$$

where the zero-order correlation function $C(t) = \langle D_{00}^2[\theta(0)]D_{00}^2[\theta(t)]\rangle$ can be readily calculated from a MD trajectory using the Wigner rotation matrix.

The MD trajectories for this work were obtained from constant-NVT simulations on a single solute probe molecule (Fig. 1) in a CG liquid crystalline solvent. We employed the methodology used in previous MD simulations [19,20]. In brief, the simulations used the AMBER all-atom force field for the probe molecule, with additional charges

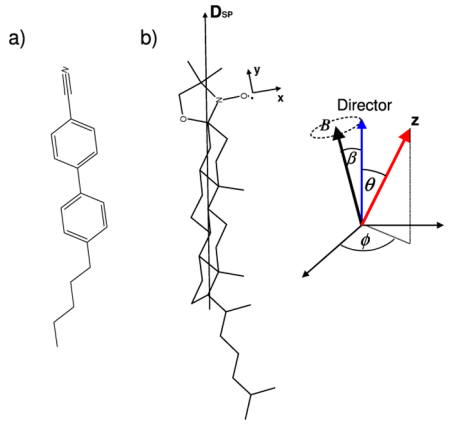

FIG. 1 (color online). Molecular structures of 5CB mesogen (a) and cholesteric nitroxide spin probe (b). The orientation of x, y, and z axes of the magnetic frame together with the long rotational diffusion axis of spin probe $\mathbf{D}_{SP}$ are indicated.

for the head group taken from a density functional theory B3LYP//6-31G(d, p) study using a CHELPG scheme [21], in conjunction with a cut and shifted Gay-Berne (GB) model ($\kappa = 3.0$, $\kappa' = 5$) to describe the mesogen [22]. A value of $\sigma_{GB} = (2)^{1/2}d_{GB} = 4.721$ Å was used (estimated from the dimensions of the mesogenic unit) to scale the GB particle to real units, and four simulations were prepared corresponding to a reduced solvent density of $\rho^* = 0.321\,85$ using different values for the GB well depth, $\epsilon_{GB}/k_B = 302.86, 205.63, 176.26, 156.00$ K. These were respectively simulated at temperatures of 25 °C, 35.3 °C, 35.3 °C, and 39 °C, corresponding to reduced solvent temperatures of $T^* = k_BT/\epsilon_{GB}$ for state points where the system is nematic ($T^* = 0.984$), isotropic ($T^* = 2.0$), and almost at the nematic-isotropic (N-I) transition (for $T^* = 1.5, 1.75$). The EPR spectra of nitroxide spin probes were determined entirely by the variation in time of two angles that define the orientation of the applied magnetic field to the principle axis of the nitroxide group. Therefore, the orientational history of the z axis of the nitroxide ring (the direction of p orbital of N) was calculated from MD output as the cross product of the unit vectors of N-O and N-C bonds.

In order to provide experimental validation of the method, EPR spectra of LC samples with introduced spin probe were measured using an X-band (9.5 GHz) cw Bruker Elexsys E500 spectrometer. A concentration of ~0.2 mM nitroxide spin label 3β-DOXYL-5α-cholestane, CSL (Aldrich) in 4-n-pentyl-4′-cyanobiphenyl, 5CB (Merck KGaA) was achieved by mixing their dichloromethane solutions. After dichloromethane solvent was evaporated by heating the mixture up to 320 K, the latter was injected into the 0.3 mm diameter quartz tube and placed into the X-band Bruker spectrometer.

For the system studied, separate orientational order parameters can be defined for the LC mesogens and the

probe. The order parameter for a particular molecular vector **u** can be found by diagonalizing the ordering tensor $Q_{ij} = \langle \frac{1}{2}(3u_i u_j - \delta_{ij})\rangle$ and taking the largest eigenvalue as the instantaneous order parameter with the corresponding eigenvector yielding the director. For 5CB, **u** is the vector which defines the long molecular axis of the 5CB mesogen. In the case of paramagnetic probe there are two ordering tensors and associated order parameters related to the dynamics of the spin probe. The first one is defined by the vector associated with the rigid part of the probe ($\mathbf{u} = \mathbf{D}_{SP}$; S_{SP} spin probe's order parameter). The second one is defined by the magnetic axis of the nitroxide head group ($\mathbf{u} = \mathbf{y}$; S_Y order parameter) (see Fig. 1).

The *N*-*I* phase transition for 5CB occurs at 35.3 °C. In the experimental EPR sample the director is not perfectly aligned in the *N* phase but characterized by an axial anisotropic distribution around the direction of magnetic field [9]. The director's distribution bandwidth of $\sim 15^0$ is in agreement with the fit obtained using the traditional Brownian dynamics simulation model as implemented in EPRSSP_DYN EPR simulation program [7]. Principle values of **g** and **A** tensors, namely, $A_{xx} = 5.9$ G, $A_{yy} = 5.9$ G, $A_{zz} = 31.7$ G and $g_{xx} = 2.0088$, $g_{yy} = 2.0061$, $g_{zz} = 2.0027$ for the spin probe dissolved in 5CB LC were taken from the literature [9,23].

Figure 2 shows EPR spectra predicted from MD simulations carried out at different temperatures. Simulations of nematic and isotropic phases are in excellent agreement with the available experimental data. As an example, the autocorrelation function of the *z* magnetic axis obtained from MD simulation of nematic phase is shown in Fig. 3. An associated MD trajectory used to predict the EPR spectrum [Fig. 2(*a*)] is shown in the subplot. Analysis has demonstrated that longer trajectories provide virtually indistinguishable results. This is because the correlation times of spin-label reorientational dynamics calculated according to (6) appear to be less then 0.1 ns, making all statistical averages achievable at relatively short time scales.

In the nematic phase, the EPR spectrum consists of three broad closely positioned hyperfine lines. As the temperature increases, two distinct changes in the spectra are taking place: (i) the lines get narrower, (ii) the distances among them increase and approach their isotropically averaged positions. These changes in EPR spectra can be easily explained from the analysis of MD results. The statistical distribution of the magnetic *z* axis on a unit sphere (Fig. 2) indicates that in the nematic phase (a) the spin probes's dynamics is highly anisotropic with the position of the *z* axis being on average perpendicular to the director's and field orientation. For perpendicular orientation of the *z* axis relative to the magnetic field ($\theta = 90^0$), the distance between the resonance field positions of $m = 1$ and $m = -1$ hyperfine lines is $\sim 2A_{xx/yy}$, which corresponds very closely to the distance between the right and left crossover points observed in the spectra (*a*) of

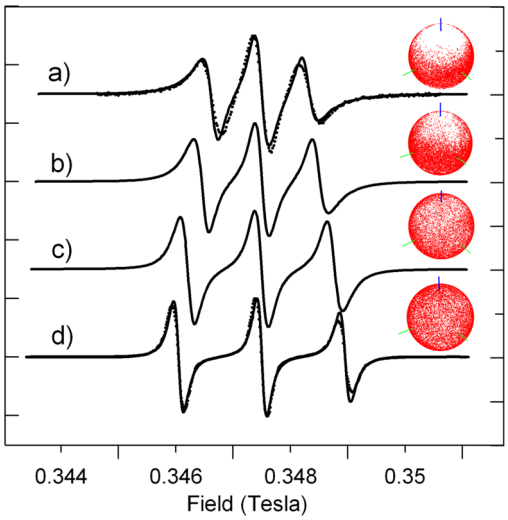

FIG. 2 (color online). *X*-band EPR spectra predicted from MD calculations carried out at four different regimes (solid lines): (*a*) nematic phase ($T = 25$ °C), (*b*) and (*c*) *N*-*I* phase transition ($T = 35.3$ °C) as approached from *N* and *I* starting configurations, respectively, and (*d*) isotropic phase ($T = 39$ °C). Distributions of magnetic *z* axis on a unit sphere (points accumulated during the 20 ns runs) are shown for each spectrum. Available experimental EPR spectra are shown by dotted lines. EPR spectrum corresponding to isotropic phase (*d*) is taken from the literature [9]. In the simulations $T_2^m = 0.18$ μs and 0.25 μs for (*a*),(*b*) and (*c*),(*d*), respectively.

Fig. 2. Upon approaching the *N*-*I* phase transition from either *N* or *I* equilibrated states, changes in EPR are observed which exhibit "mixed" patterns of motion and order of the probe [(*b*) and (*c*)]. In the pure isotropic state, because of the fast dynamics of the spin probe, the hyperfine coupling and the *g* tensor are completely averaged and the distance between the crossover points increases to the value of $\sim 2/3(A_{xx} + A_{yy} + A_{zz})$. At the same time all order parameters approach zero values.

The values of different order parameters in each state calculated from MD trajectories are shown in Table I. The *y* magnetic axis and the long diffusion axis of the probe are nearly collinear with the estimated angle between them of less then 15° [9]. In this case for the magnetic axes of the probe, $S_Z \sim -1/2S_Y$, as expected for a uniaxial particle in a uniaxial phase. The values of the order parameters for both LC and the main diffusional axis of the probe, S_{LC} and S_{SP}, respectively, as well as the values of rotational diffusion coefficients, calculated from the correlation times are in excellent agreement with those reported in the literature [9]. According to Table I strong correlation among the four order parameters is evident. At the same time, the observed differences among their values can be easily explained. First, because the spin probe molecule is slightly longer then the solvent one we would expect it to have slightly larger order parameter. Second, the nitroxide head group has higher degree of mobility compared to the core of the

TABLE I. Order parameters for different MD calculations described in Fig. 2.

LC state	S_{LC}[a]	S_{SP}[b]	S_Y[c]	S_Z[c]	τ_c/ns[d]
(*a*)	0.71	0.75	0.46	0.21	0.035
(*b*)	0.48	0.52	0.26	0.13	0.040
(*c*)	0.27	0.27	0.12	0.05	0.030
(*d*)	0.10	0.05	0.02	0.01	0.015

[a]Order parameter for LC mesogens.
[b]Order parameter for spin probe.
[c]S_Y and S_Z are order parameters associated with the magnetic y and z axes of the nitroxide head group, respectively.
[d]τ_c is the correlation time for the reorientational dynamics of magnetic z axis calculated according to Eq. (6).

probe resulting in a lower order parameter. In addition, the z axis being on average perpendicular to the director has high degree of mobility, compared to y, which results in the lowest values for the corresponding order parameter.

In summary, we have carried out the first successful simulation of LC EPR spectra directly and entirely from generated MD trajectories. Our procedure does not require additional modeling for spin probe's dynamics with adjustable parameters and, therefore, provides better understanding of dynamics and order of molecules, allowing easier interpretation of the spectra and, ultimately, saving analysis time. More importantly, simulation of EPR spectra directly from molecular structures opens the possibility of ''computer engineering'' of spin-labeled materials with the desired properties prior to experiment. For example, in biology this should allow the prediction of sites for spin label attachment by site directed mutagenesis that will produce the required level of orientation and mobility

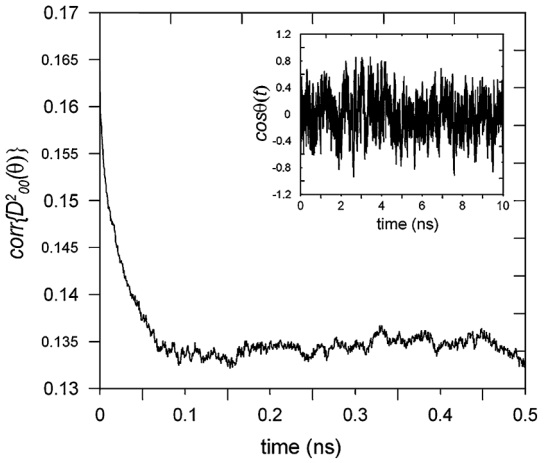

FIG. 3. Autocorrelation function for the θ angle between magnetic z axis of the nitroxide probe and the director in the nematic phase of 5CB [$D^2_{00} = (3\cos^2\theta - 1)/2$]. MD trajectory used in the simulation of EPR spectrum (*a*) in Fig. 2 is shown in the subplot.

to study a particular problem. Results show that for the motional time range of a SP, introduced within 5CB, a 10 ns MD trajectory was sufficiently long to achieve excellent agreement with experiment. EPR spectra predicted from MD simulations show strong sensitivity to the changes in order and dynamics of mesogens associated with the phase transition making the combination of EPR with MD simulations a powerful tool to study LC systems.

V. S. O. thanks the EPSRC for financial support (Grants GR/T01754/01 and GR/T01761/01) and The Wellcome Trust for funding the Henry Wellcome Unit for Biological EPR.

*V.oganesyan@uea.ac.uk

[1] L. J. Berliner, *Spin Labeling: The Next Millennium* (Plenum, New York, 1998).
[2] W. L. Hubbell, D. S. Cafiso, and C. Altenbach, Nat. Struct. Biol. **7**, 735 (2000).
[3] P. P. Borbat, A. J. Costa-Filho, K. A. Earle, J. K. Moscicki, and J. H. Freed, Science **291**, 266 (2001).
[4] R. D. Nielsen, K. P. Che, M. H. Gelb, and B. H. Robinson, J. Am. Chem. Soc. **127**, 6430 (2005).
[5] B. J. Gaffney and D. Marsh, Proc. Natl. Acad. Sci. USA **95**, 12 940 (1998).
[6] P. Z. Qin, K. Hideg, J. Feigon, and W. L. Hubbell, Biochemistry **42**, 6772 (2003).
[7] G. F. White, L. Ottignon, T. Georgiou, C. Kleanthous, G. R. Moore, A. J. Thomson, and V. S. Oganesyan, J. Magn. Reson. **185**, 191 (2007).
[8] M. Zachary and V. Chechik, Angew. Chem., Int. Ed. **46**, 3304 (2007).
[9] A. Arcioni, C. Bacchiocchi, I. Vecchi, G. Venditti, and C. Zannoni, Chem. Phys. Lett. **396**, 433 (2004).
[10] G. R. Luckhurst, Thin Solid Films **509**, 36 (2006).
[11] D. A. Case, Acc. Chem. Res. **35**, 325 (2002).
[12] M. R. Wilson, Int. Rev. Phys. Chem. **24**, 421 (2005).
[13] D. E. Budil, K. L. Sale, K. A. Khairy, and P. G. Fajer, J. Phys. Chem. A **110**, 3703 (2006).
[14] C. Beier and H. J. Steinhoff, Biophys. J. **91**, 2647 (2006).
[15] B. H. Robinson, L. J. Slutsky, and F. P. Auteri, J. Chem. Phys. **96**, 2609 (1992).
[16] I. Stoica, J. Mol. Model. **11**, 210 (2005).
[17] V. S. Oganesyan, J. Magn. Reson. **188**, 196 (2007).
[18] H. J. Steinhoff and W. L. Hubbell, Biophys. J. **71**, 2201 (1996).
[19] M. R. Wilson, J. M. Ilnytskyi, and L. M. Stimson, J. Chem. Phys. **119**, 3509 (2003).
[20] M. R. Wilson, L. M. Stimson, and J. M. Ilnytskyi, Liq. Cryst. **33**, 1167 (2006).
[21] C. M. Breneman and K. B. Wiberg, J. Comput. Chem. **11**, 361 (1990).
[22] J. T. Brown, M. P. Allen, E. M. del Rio, and E. de Miguel, Phys. Rev. E **57**, 6685 (1998).
[23] E. Meirovitch and J. H. Freed, J. Chem. Phys. **88**, 4995 (1984).